

CONSTRAINING ATMOSPHERIC DUST LIFTING ON DIURNAL TIMESCALES FROM EMIRS SURFACE TEMPERATURE OBSERVATIONS

C. A. Wolfe, Northern Arizona University, Flagstaff, AZ, USA (cw997@nau.edu), C. S. Edwards, Northern Arizona University, Flagstaff, AZ, USA, M. D. Smith, NASA Goddard Space Flight Center, Greenbelt, MD, USA, M. J. Wolff, Space Science Institute, Boulder, CO, USA.

Introduction: Regional and planet-encircling dust storms occur episodically on Mars, influencing the thermal structure and dynamics of the atmosphere. While suspended dust particles are nearly always present in the atmosphere of Mars at some background level, conditions may arise that promote vigorous dust lifting to occur and existing local or small-scale dust storms to grow or coalesce, obscuring vast regions of the planet in a thick dust for periods ranging from a few days to many weeks [1]. When dust storms occur, they often alter atmospheric circulation [2, 3, 4, 5, 6, 7, 8], change surface albedo patterns [9, 10, 11] and modify subsequent transport and deposition of water and CO₂ at the poles [12, 13, 14]. Dust storms, regardless of their scale, are a key aspect of the Martian dust cycle. While a community effort is being put forth to characterize the conditions necessary for the onset, growth, and decay of dust storms, little is still known about their diurnal variability.

Most quantitative dust measurements from orbiters during global dust storm events have provided dust column amounts that are available only on the dayside part of the orbit [15]. The highly elliptical orbit of the Emirates Mars Mission (EMM) spacecraft [16] along with fortuitous regional dust storm event that occurred near the end of 2021 provide a unique opportunity to investigate atmospheric dust lifting on diurnal timescales. Using a numerical thermal model and Emirates Mars Infrared Spectrometer (EMIRS) surface temperature observations, an upper limit (in μm) will be placed on the amount of dust that was lofted from the surface before, during, and after the regional dust storm that occurred near Syrtis Major. Results from EMIRS observations will be compared to those made by the Thermal Imaging System (THEMIS) instrument on-board Mars Odyssey during the same time to help further constrain dust lifting. Together, these measurements will assist in our understanding of dust storm growth and evolution on diurnal timescales.

Dataset: Syrtis Major is a well-known dark feature lying between the boundary of the northern lowlands and southern highlands of Mars. The dark, low albedo color is the result of basaltic lava flows covering much of ancient, gently-sloping shield volcano. The region often undergoes changes in appearance [10], with the width of the dark region exhibiting both seasonal and long-term variations [17, 18]. The-

se changes have been attributed to a brightening caused by global dust storms, followed by darkening caused by dust removal through aeolian processes [19, 20].

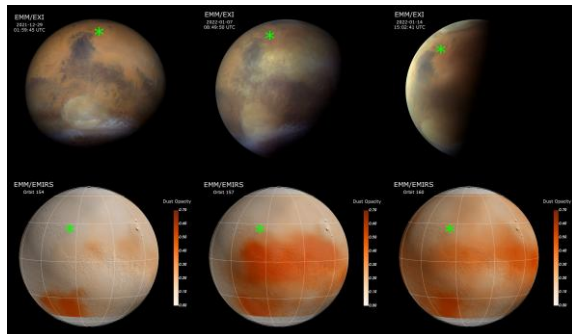


Figure 1: EXI (top) and EMIRS (bottom) observations showing the evolution of column dust optical depth from several regional dust storms occurring near the end of 2021.

Starting in December 2021, the Emirates Exploration Imager (EXI) and EMIRS instruments monitored a rapidly-evolving regional dust storm as it grew in size (see Figure 1). On December 29, 2021 (L_S 149°; EMM orbit number 154), EXI captured a fully illuminated disk of Mars centered near Syrtis Major. As is typical for southern hemisphere winter, the atmosphere was relatively clear, with only a few discrete water-ice clouds visible over the plains east of Syrtis Major. Over the next two weeks, both EXI and EMIRS show high concentrations of airborne dust approaching and obscuring much of the Syrtis Major region. During this time, EMIRS observations reveal a significant increase in the thickness of the diffuse dust haze, suggesting the active lifting of dust from the surface.

Methodology: The depletion and replenishment of surface dust reservoirs available for dust storm onset and growth leaves a measurable thermophysical signature (i.e. thermal inertia, albedo) that we will quantify using EMIRS surface temperature observations. Variations in diurnal surface temperature will be interpreted in terms of addition or removal of surface dust on an otherwise coarser regolith. Atmospherically corrected surface temperatures are retrieved using the 15- μm CO₂ absorption band [21].

Employing the KRC numerical thermal model [22], a variety of layered surface and subsurface

conditions are simulated to produce a multi-dimensional lookup table. Specifically, we are interested in modeling the removal of a thin layer of fine-grained, low thermal inertia, high albedo dust particles on top a substrate with a higher bulk thermal inertia and lower albedo [23]. Using a host of input parameters, including L_S , latitude, local time, elevation, and dust opacity, surface temperature is derived for a variety of thermal inertia and surface albedo values, allowing different dust layer thicknesses to be modeled.

Surface temperature is modeled as a function of local time based on data collected near the center of the Syrtis Major quadrangle (10° N, 60° E). To compute the surface temperature difference and thus constrain the amount of dust that was lifted during the dust storm, modeled diurnal surface temperature curves were subtracted from one another. This simple algebraic operation was performed for several cases, including instances where either surface albedo or thermal inertia were allowed to vary, with the other remaining input parameters held constant. Figure 2 demonstrates the effect a variety surface and subsurface conditions have on surface temperature difference over diurnal time scales.

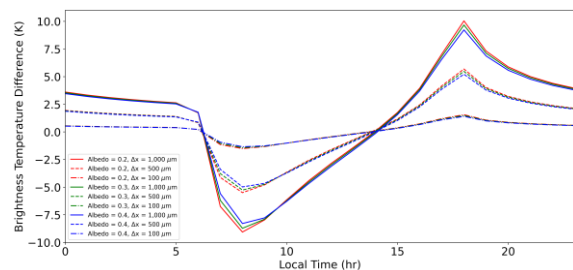


Figure 2: Modeled diurnal surface temperature difference curves for the Syrtis Major region demonstrating the influence of albedo and dust thickness.

Using the Java Mission-planning and Analysis for Remote Sensing (JMARS) software suite [24], a query was performed that returned EMIRS pixels occupying the Syrtis Major region (approximately a $13^\circ \times 31^\circ$ rectangular grid) based on EMM orbit number. Only pixels that were acquired with the center detector were utilized as this detector was found to have the highest performance. Furthermore, the query restricted returning any pixels with an emission angle exceeding 70° . Retrieved parameters, including brightness temperature and column dust optical depth, were exported to a tabulated CSV file. A Python script was written to ingest the CSV files that were generated and bin the retrieved parameters by 15-minute local time intervals. The average value of the retrieved parameter of interest was then computed for each local time bin.

The JMARS query described above was carried out for a total of 7 EMM orbits (Orbit number 153, 154, 156, 157, 158, 165, 166), with surface tempera-

ture difference derived from EMIRS data acquired before and after the dust storm event. The surface temperature difference resulting from dust lifting depends strongly on the time of day, with surface temperature decreases typically occurring during the day and increases during the night. The surface temperature fluctuations induced by dust removal are largely due to the thermal properties of the dust and underlying surface material, specifically their thermal inertias. As the fine grain, low thermal inertia dust is lifted aloft through various mechanisms, it exposes the coarse, high thermal inertia surface material below. To place an upper limit on the amount of dust lifted or removed from the surface, modeled diurnal surface temperature difference curves from KRC are compared with EMIRS observations.

Preliminary Results:

Figure 3 illustrates the binned and averaged diurnal surface temperature differences determined from EMIRS data acquired before and after the dust storm event. Due to both local time coverage and the binning method, data is somewhat sparse during the morning and evening hours. Furthermore, the observed data exhibits a high degree of variability, which may stem from the rather large region of interest sampled. Despite the sporadic nature of the data points, there does appear to be some weak agreement with the modeled data from KRC, specifically a temperature decrease during the daytime hours and an increase during the nighttime hours.

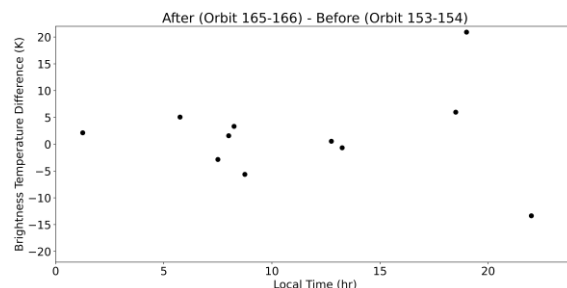


Figure 3: Binned and averaged diurnal surface temperature differences based on EMIRS surface temperature data before (EMM orbits 153-154) and after (EMM orbits 165-166) the dust storm event.

Summary and Future Work:

We have successfully demonstrated the ability to place upper limits on the amount of dust lifted from the surface of Mars following a regional dust storm. While the observed EMIRS surface temperature data between successive EMM orbits shows significant variability, we find some agreement with surface temperature differences modeled with KRC. Future work will involve reducing the variability in EMIRS surface temperature data, perhaps through refining the selected region of interest, to constrain dust lifting with a greater degree of accuracy.

References:

- [1] Martin, L. J., and Zurek, R. W. (1993), An analysis of the history of dust activity on Mars, *J. Geophys. Res.*, 98(E2), 3221–3246.
- [2] Conrath, B. J. (1975). Thermal structure of the Martian atmosphere during the dissipation of the dust storm of 1971. *Icarus*, 24(1), 36–46.
- [3] Guzewich, S. D., Wilson, R. J., McConnochie, T. H., Toigo, A. D., Banfield, D. J., & Smith, M. D. (2014). Thermal tides during the 2001 Martian global-scale dust storm. *Journal of Geophysical Research: Planets*, 119, 506–519.
- [4] Haberle, R. M., Leovy, C. B., & Pollack, J. B. (1982). Some effects of global dust storms on the atmospheric circulation on Mars. *Icarus*, 50(2-3), 322–367.
- [5] Leovy, C. B., & Zurek, R. W. (1979). Thermal tides and Martian dust storms: Direct evidence for coupling. *Journal of Geophysical Research*, 84(B6), 2956–2968.
- [6] Newman, C. E., Lewis, S. R., Read, P. L., & Forget, F. (2002). Modeling the Martian dust cycle, 1. Representations of dust transport processes. *Journal of Geophysical Research*, 107(E12), L04203.
- [7] Wilson, R. J. (1997). A general circulation model simulation of the Martian polar warming. *Geophysical Research Letters*, 24(2), 123–126.
- [8] Zurek, R. W. (1982). Martian great dust storms: An update. *Icarus*, 50(2–3), 288–310.
- [9] Cantor, B. A. (2007). MOC observations of the 2001 Mars planet-encircling dust storm. *Icarus*, 186(1), 60–96.
- [10] Szwest, M. A., Richardson, M. I., & Vasavada, A. R. (2006). Surface dust redistribution on Mars as observed by the Mars Global Surveyor and Viking orbiters. *Journal of Geophysical Research*, 111, E11008.
- [11] Vincendon, M., Audouard, J., Altieri, F., & Ody, A. (2015). Mars Express measurements of surface albedo changes over 2004–2010. *Icarus*, 251, 145–163.
- [12] Benson, J. L., & James, P. B. (2005). Yearly comparisons of the Martian polar caps: 1999–2003 Mars Orbiter Camera observations. *Icarus*, 174(2), 513–523.
- [13] Cantor, B. A. (2007). MOC observations of the 2001 Mars planet-encircling dust storm. *Icarus*, 186(1), 60–96.
- [14] Strausberg, M. J., Wang, H., Richardson, M. I., Ewald, S. P., & Toigo, A. D. (2005). Observations of the initiation and evolution of the 2001 Mars global dust storm. *Journal of Geophysical Research*, 110, E02006.
- [15] Kleinboehl, A., Spiga, A., Kass, D. M., Shirley, J. H., Millour, E., Montabone, L., & Forget, F. (2020). Diurnal variations of dust during the 2018 global dust storm observed by the Mars Climate Sounder. *Journal of Geophysical Research: Planets*, 125, E006115.
- [16] Amiri, H.E.S., Brain, D., Sharaf, O. et al. The Emirates Mars Mission. *Space Sci Rev* 218, 4 (2022)
- [17] Sagan, C., Veverka, J., Fox, P., Dubisch, R., French, R., Gierasch, P., Quam, L., Lederberg, J., Levinthal, E., Tucker, R., Eross, B., Pollack, J. B., (1973) *Journal of Geophysical Research*, 78(20), 4163-4196.
- [18] McKim, R. J. (1999). Telescopic Martian dust storms: a narrative and catalogue. *Memoirs of the British Astronomical Association*, 44, 165.
- [19] Lee, S. W. (1986). Regional sources and sinks of dust on Mars; Viking observations of Cerberus, Solis Planum, and Syrtis Major, *LPI Contribution* 599: 57-58.
- [20] Christensen, P. R. (1988). Global albedo variations on Mars: Implications for active aeolian transport, deposition, and erosion, *J. Geophys. Res.*, 93(B7), 7611–7624.
- [21] Edwards, C.S., Christensen, P.R., Mehall, G.L. et al. The Emirates Mars Mission (EMM) Emirates Mars InfraRed Spectrometer (EMIRS) Instrument. *Space Sci Rev* 217, 77 (2021).
- [22] Kieffer, H. H. (2013), Thermal model for analysis of Mars infrared mapping, *J. Geophys. Res. Planets*, 118, 451–470.
- [23] Edwards, C. S., Nowicki, K. J., Christensen, P. R., Hill, J., Gorelick, N., and Murray, K. (2011), Mosaicking of global planetary image datasets: 1. Techniques and data processing for Thermal Emission Imaging System (THEMIS) multi-spectral data, *J. Geophys. Res.*, 116, E10008.
- [24] Christensen, P. R., et al. (2009) JMARS - A Planetary GIS, American Geophysical Union, Fall Meeting 2009.